



IJSRM

INTERNATIONAL JOURNAL OF SCIENCE AND RESEARCH METHODOLOGY

An Official Publication of Human Journals



Human Journals

Research Article

May 2024 Vol.:27, Issue:5

© All rights are reserved by Bertrand Tsouongang et al.

Enhance the Performance of Activated Carbon Obtained from Biomass Waste for the Adsorption of Yellow 145 in Aqueous Media



IJSRM

INTERNATIONAL JOURNAL OF SCIENCE AND RESEARCH METHODOLOGY

An Official Publication of Human Journals



Bertrand Tsouongang¹, Jules Leuna Mabou¹, Judith Maffeu¹, Suzanne Makota¹, Harlette Poumve Zapenaha¹, Mariame Conde¹, Pierre Gerard Tchieta^{1*}

¹Department of Chemistry, Faculty of Science, University of Douala, Douala P.O. Box 24157, Cameroon

Submitted: 20 April 2024

Accepted: 26 April 2024

Published: 30 May 2024



HUMAN JOURNALS

ijsrm.humanjournals.com

Keywords: Adsorption, activated carbon, Composite, Nanoparticle, Yellow 145.

ABSTRACT

This study aims to synthesize a composite with enhanced adsorption properties by incorporating zinc oxide into activated carbon derived from snail shells, chemically activated with zinc acetate, to reduce Yellow 145 in aqueous media. The composite was synthesized by converting snail shells into activated carbon through chemical activation. The reduction of Zinc oxide nanoparticles was done directly in the porosity of activated carbon and the material obtained were called **ZnONPs-AC** (Zinc Oxide Nanoparticles landed with activated carbon). The composite was characterized using pH zero charge point (pHZPC), iodine number, methylene blue number, X-ray diffraction (XRD), Fourier Transform Infrared Spectroscopy (FT-IR), Scanning Electron Microscopy (SEM), and Energy Dispersive X-ray Spectroscopy (EDX). These techniques confirmed the semicrystalline nature of the composite, with mixed micro- and mesoporosity and the presence of ZnONPs on its surface. Various parameters have been studied and show the high performance of the composite. The pseudo-second-order and intraparticle diffusion models indicated that the adsorption of Yellow 145 occurred primarily through intra-particle diffusion within the pores of the activated carbon. Four isotherm models were studied, with the Freundlich isotherm best describing the adsorption mechanism. This was further supported by the Dubinin-Radushkevich (DRK) isotherm, indicating physical adsorption due to lower activation energy.

INTRODUCTION

Water is a precious natural resource that is indispensable to human and plant existence. Without it, there can be no life, agriculture or industrial development on earth. Water is a crucial element that must be preserved during economic growth in order to respect the environment - indeed, it is one of the UN's Sustainable Development Goals (SDGs), to be achieved by 2030 [1]. With the proliferation of industrial activities, water has become a commodity highly exposed to pollution.

In fact, water pollution can be defined as the modification of its physical and chemical properties by the introduction of a polluting element, which may originate from anthropogenic activities, i.e. human activities, agricultural activities and industrial activities [2]. Many industries, such as cosmetics, pharmaceuticals, textiles and printing, use various dyes to color and give their products a good appearance [3, 4]. However, when these dyes are handled, large quantities are released into water. Yellow 145 is carcinogenic and toxic to humans and animals [5, 6]. The toxicity of yellow 145 is not new. From 1895, the increase in the number of bladder cancers observed in textile industry workers was due to their prolonged exposure to azo dyes because yellow 145 is an azo dye [5]. This dye is widely used because of its low cost, making it a popular choice for textile dyeing. Faced with the critical situation of water pollution by dyes and the growing collective awareness of this issue, research in the field of depollution is progressing rapidly, the aim being to develop the most robust, economically feasible, easy-to-use, sustainable and environmentally-friendly methods of depollution.

Several water treatment methods are available for depolluting the aqueous environment. They include physical treatment (screening, decantation, filtration, flotation, and adsorption); chemical (oxidation, ion exchange on resin, neutralization or acidification processes); physical-chemical (coagulation-flocculation), and biological (appropriate bacterial cultures) [7]. Among these methods, adsorption is one of the best alternative methods, economically attractive for wastewater treatment because of its convenience, ease of use, simplicity of design and effectiveness [8, 9]. Adsorption is a process during which pollutant molecules in an aqueous medium bind to the surface of a solid adsorbent material [10]. The most commonly used adsorbents for pollution control are: silica gel, activated alumina, activated clay, zeolite and activated carbon, which is the most effective due to its high adsorption capacity due to its large specific surface area [11]. Activated carbon can be synthesized from plant or animal biomass

waste such as peanut shells, sawdust, rice husks, cotton stalks, eucalyptus bark, mango kernel, almond shells and snail shells [12, 13]. The strongest biomasses may be able to produce efficient activated carbons. Among many other precursors of activated carbon, snail shell has several important uses, which result from its hard nature. Recent development involves its application in wastewater treatment due to its chemical composition; this composition includes proteins, carbohydrates, fats and minerals such as iron, zinc, copper. Activated carbon is prepared in several stages: precursor harvesting, precursor pre-treatment (washing, drying, grinding and sieving), activation and carbonization (thermal decomposition of carbonaceous materials, during which species other than carbon are eliminated) [14]. Activation consists in impregnating the precursor powder with an activating reagent to ensure better development of the specific surface area and porous structure obtained after the carbonization stage, by eliminating pore-clogging impurities and increasing chemical functions on the activated carbon surface [15]. However, two activation methods are commonly used: physical activation and chemical activation. Physical activation involves oxidation of the precursor at high temperature (800 to 1000°C) using weakly oxidizing activating agents (air, steam and carbon dioxide) for 24 to 72 hours [16]. In contrast to physical activation, chemical activation is carried out simultaneously with the carbonization step at a relatively low temperature (400 to 800°C) in the presence of chemical activating reagents such as phosphoric acid, sulfuric acid, potassium sulfide, zinc chloride, copper salts or potasse [17, 18].

Although activated carbon is a model adsorbent for wastewater treatment due to its high specific surface area, it has limitations due to its low reaction rate, low reusability and difficult regeneration [19]. With the aim of improving this treatment technique, researchers in the field are using nanoparticles that they incorporate into activated carbon to form composite materials, since nanoparticles are highly reactive and interact immediately upon injection into the polluted aqueous medium with the pollutant molecules, and can be applied several times without losing their effectiveness [20, 21]. Zinc oxide nanocomposites have already been used for the adsorption of several pharmaceutical compounds and many other industrial pollutants, and data have shown them to be highly effective adsorbents for the decontamination of aqueous media [22, 23]. Zinc oxide is non-toxic and easy to obtain. In addition, it is a nanoparticle whose structure is unaffected by climate change [24]. The high binding energy (60 M eV) of zinc oxide has made it a highly exploited nanoparticle by researchers, as it establishes strong chemical

bonds on the basic adsorbent material, activated carbon [25]. Zinc oxides have a number of advantages over other metal oxides such as Fe_2O_3 , TiO_2 and SiO_2 , not least of which is their stoichiometry. Zinc oxides offer various advantages over other metal oxides such as Fe_2O_3 , TiO_2 , and SiO_2 , notably their unique thermal stability, chemical stability and long shelf life [26]. In this study, we will synthesize an activated carbon by chemical activation with zinc acetate, and incorporate zinc oxide nanoparticles to form a composite material to enhance its performance.

I. Materials, reagents and protocol used

This part consists of presenting the materials and reagents that we used for the preparation of activated carbon and the characterization of composite. Materials as balance, crucibles, beakers, a graduated pipette, a washbowl, a spatula, a graduated burette, an Erlenmeyer flask, volumetric flasks, magnetic stirrers (heated and unheated) and bar magnets, an oven, a grinder, a probe thermometer, UV-Visible absorption spectrophotometry, filter paper Whatman number 5, a pH meter and an oven. Reagents used include methylene blue, iodine, potassium iodide, sodium thiosulfate, sodium chloride, hydrochloric acid, sodium hydroxide, yellow 145, zinc oxide, zinc acetate.

I.2 Methodology

I.2.1. Preparation of activated carbon

The snail shells were washed abundantly with distilled water in order to eliminate all traces of impurities, then air-dried for 05 days in order to eliminate all traces of water in the precursor. Once this stage was completed, the snail shells were mechanically crushed using a hammer, then crushed in a suitable machine. The resulting powder was mechanically sieved using a $63\ \mu\text{m}$ diameter sieve to obtain a uniform particle size. This powder was then impregnated with zinc acetate hydrate $(\text{CH}_3\text{COO})_2\text{Zn} \cdot 2\text{H}_2\text{O}$; Then 50g of powder was brought into contact with 200 ml of a 0.3 mol/l $(\text{CH}_3\text{COO})_2\text{Zn} \cdot 2\text{H}_2\text{O}$ solution, then the mixture was stirred magnetically at room temperature for 2 h, then dried in an oven at 105°C for 24 h. Our impregnated precursor was then calcined in an electric furnace at a maximum temperature of 500°C , with a heating rate of $5^\circ\text{C}/\text{min}$ and a residence time of 2 h at this maximum temperature [27]. After removal from the furnace, we used a porcelain mortar to crush the activated carbon to

a fine powder, then washed it with deionise water until the washing pH was neutralized. Finally, our AC was oven-dried at 105°C for 24 hours, then stored for future use.

I.2.2. Preparation of the composite activated carbon landed with zinc oxide nanoparticle (ZnONPs-AC)

Our composite was synthesized by direct incorporation under magnetic stirring. To this end, we prepared an aqueous solution of zinc oxide at a concentration of 0.3 mol/L. 100 ml of this solution was brought into contact with 20 g of activated carbon, then stirred magnetically for 2h. We then introduced a sodium hydroxide solution at a concentration of 0.1 mol/L as a reducing agent, and stirred the whole mixture for 2h; after stirring, the final material was filtered, washed thoroughly with deionise water, then dried at 105°C in an oven for 24h and stored for future use. Our composite was designated ZnONPs-AC.

I.3 Characterization of our composite

I.3.1 pH at the zero point of charge pHZPC

The pH of the point of zero charge (pHZPC), is the pH for which the surface of the solid has a zero charge; its role is to determining the acid-basic character of a material. Adsorbent and pollutant chemistry in aqueous solution depends to some extent, invariably, on pH of the environment. Consequently, pH of the material is an important parameter taken into account in this study. It was determined by introducing 0.1 g of adsorbent previously dried with 20 mL of a decimal solution of NaCl into different Meyer flasks. pH of the solutions was adjusted between 2 and 10 (pHi) initial pH using a pH meter (pHS-3C) using decimal solutions of NaOH and HCl, then stirred for 72 hours at room temperature [28]. After stirring, the resulting solutions were filtered and the pH of the filtrates was measured (pHf). The difference between pHi and pHf ($\Delta pHi - \Delta pHf$) is plotted against pHi. The point of intersection between the curve and the x-axis corresponds to the pH at the zero-charge point (pHZPC).

I.3.2 Iodine value

The iodine value in (mg/g) is an indicator of a material's capacity to adsorb very small molecules. The iodine index test was carried out using the following protocol: in the 100 mL Erlenmeyer flask, a 0.1 g mass of our composite was brought into contact with a 20 mL volume of the 0.02 N normality iodine solution. The mixture was stirred at room temperature for 1 hour. It was then filtered through Whatman paper number 5, 10 mL of the filtrate was assayed with sodium thiosulfate (Na₂S₂O₃) solution of normality 0.1 N in the presence of three drops of starch employment [29, 30]. The iodine value is given by the following relationship:

$$Indice\ d'iode = \frac{(C_0 - \frac{C_{thio} \times V_{thio}}{2V_{I_2}}) M_{I_2} \times V_{ads}}{m_{ZnONPs-AC}} \dots\dots\dots 1$$

C₀ initial concentration of I₂, C_{th} concentration of Na₂S₂O₃, V_{th} volume of Na₂S₂O₃ poured at equivalence, V_{I₂} volume of I₂ dosed, M_{I₂} molar mass of I₂, V_{ads} adsorption volume, m ZnONPs-AC mass of activated carbon.

I.3.3. Methylene blue index

The methylene blue number (MB), expressed in mg/g, represents the adsorption capacity of the material for medium- and large-sized molecules. To find that, the following protocol have been used. In a 250 mL beaker, 0.1g of composite have been mixed with 100mL of methylene blue solution and put under stirring for 4h [29]. After filtration, the residual MBN concentration was measured with a UV spectrometer at a wavelength λ = 620 nm. The Q (MB) and elimination rate are given by the following equations 2 and 3:

$$Q_{BM} = \frac{C_i - C_r}{m_{ZnONPs-AC}} \times V \dots\dots\dots 2$$

$$(TE\%) = \frac{C_i - C_r}{C_i} \times 100 \dots\dots\dots 3$$

Where: Q (MB) is the amount of MB adsorbed ZnONPs-AC, TE is elimination rate, V is volume of MB solution, m is the mass of ZnONPs-AC used, C_i is initial concentration of MB solution, C_r is residual concentration after adsorption.

I.3.4. Ash content determination

The ash content permit to determine the quantity of ash capable of blocking the pores of the material. In a dry crucible of mass P_1 we placed 0.1 g of composite sample and weighed P_2 . The crucible was then placed in the oven at 815°C until ash was obtained. After cooling, we weighed P_3 [29]. The ash content has been determined using the following formula:

$$(C\%) = \frac{P_3 - P_1}{P_2 - P_1} \times 100 \dots\dots\dots 4$$

I.3.5. Moisture content

The moisture content permit to determine the quantity of residual water in the material. To determine the moisture content, a mass of 0.1g of the composite was weighed and marked P_1 . This mass of composite was then introduced into a crucible and the whole was marked P_2 and placed in an oven at 110°C for 3 h. After cooling to room temperature, it was weighed and marked P_3 . After cooling to room temperature, the composite was weighed and graded P_3 [31]. The moisture content is given by the following formula.

$$(H\%) = \frac{P_2 - P_3}{P_1} \times 100 \dots\dots\dots 5$$

I.4 Adsorption test of ZnONPs-AC

Adsorption tests were carried out in batch mode. 0.01g of the composite were brought into contact with 100 mL of a solution of yellow 145 at a concentration of 100 mg/l, under magnetic stirring for a specific contact time at room temperature. After stirring, the mixtures were filtered and the filtrates were measured using a visible UV spectrophotometer at a maximum wavelength of 575 nm to determine the absorbance of the measured solutions. The quantities of pollutant absorbed at equilibrium (Q_e) per gram of ZnONPs-AC are given by the following formula 5:

$$Q_e = \frac{C_i - C_r}{m_{\text{Ca/NP-ZnO}}} \times V \dots\dots\dots 6$$

Where, Q_e is the quantity of yellow 145 adsorbed at equilibrium, V is the volume of the yellow 145 solution, m is the mass of ZnONPs-AC composite used, C_i is the initial concentration of the yellow 145 solution, C_r is the residual concentration after adsorption.

I.5. Kinetics of adsorption

The following studies determined the mechanisms as adsorption process, by pseudo-first and second order, intraparticle diffusion and Elovich diffusion. These mechanisms were used to explain the adsorption studies of yellow 145 as a function of time. The least square fit was used to obtain the various parameters. It has been studied and represented in table 1.

Table 1: nonlinear kinetic model used

Models	Equations	References
pseudo first order.	$\frac{dQ}{dt} = K_1(Q_\epsilon - Q_t)$	[32]
pseudo Second order	$\frac{t}{Q_t} = \frac{1}{K_2 Q_\epsilon^2} + (\frac{1}{Q_t})^2$	[32]
intraparticle kinetic	$Q_t = K_{id} t^{0.5} + C_i$	[33]
Elovich kinetic	$Q_t = \frac{1}{\beta \ln(\alpha\beta \times t)}$	[32]

Non-linear regression has been applied by using Excel Solver Microsoft and residual root mean square error (*RMSE*) and Chi-square test (X^2) are defined by Equations 3 and 4.

$$RMSE = \sqrt{\sum_{n=1}^n (q_{e,exp,n} - q_{e,pre,n})^2 \left(\frac{1}{n-1}\right)} \dots\dots\dots 7$$

$$X^2 = \sum_{n=1}^n \frac{(q_{e,exp,n} - q_{e,pre,n})^2}{q_{e,exp,n}} \dots\dots\dots 8$$

I.6. Modeling of adsorption isotherms

Forth isotherm models, Freundlich, Langmuir Tempkin, and Dubinin- Radushkevich (DRK) were used to evaluate the adsorption of yellow 145 on our composite material as it represents in table 2.

Table 2: Nonlinear Isotherm model used

Isotherms	Equations	References
Langmuir	$Q_{eq} = \frac{Q_{max} bC_e}{1 + bC_e}$	[34]
Freundlich	$Q_{eq} = K_F C_e^{1/n}$	[35]
Tempkin	$Q_e = \frac{RT}{b_T} \ln_{nT} C_e$	[35]
Dubinin- Radushkevich	$Q_e = Q_s e^{-\beta \epsilon^2}$	[36]

I.7. Thermodynamic parameters linked to the adsorption process

The study of the effect of temperature on adsorption allows us to determine thermodynamic parameters such as variations in enthalpy (ΔH°), standard entropy (ΔS°) and standard free energy (ΔG°) [37].

To calculate these thermodynamic parameters, we use the following equations:

$$\Delta G^\circ = \Delta H^\circ - T\Delta S^\circ \dots\dots\dots 9$$

Where ΔG is the free energy (KJ/mol), ΔH° is the enthalpy (kJ/mol), ΔS° is the entropy in (J/mol. K) and T is the temperature in kelvin.

II. Results and discussion

II.1. Instrumental characterization of our composite

II.1.1. FTIR Analysis of our materials

In order to relate the surface functions of the composite (ZnONPs-AC), they were described by FTIR spectroscopy. The figure below shows the absorption bands in the 4000 - 400 Cm^{-1} range of the Activated carbon coated of zinc oxide nanoparticles; to see all the different chemical functions present in our composite. This interpretation enables us to understand the interactions between activated carbon and zinc oxide nanoparticles (ZnONPs). We can see from Figure 1 that the presence of absorption bands at 706.20 cm^{-1} and 873.22 cm^{-1} confirms the presence of C-H bonds in the composite. These bands can be attributed to methyl (-CH3), methylene (-CH2-) or

methine (-CH-) groups present in the activated carbon [38]. The presence of absorption bands at 1402.88 cm^{-1} and 1791.84 cm^{-1} indicates the presence of oxygenated functional groups on the surface of the activated carbon. These groups can be carboxyl (-COOH) and carbonyl (-C=O) groups, which may play an important role in the interaction between activated carbon and ZnONPs [39, 40]. However, the absorption band at 1402.88 cm^{-1} and 1791.84 cm^{-1} could also correspond to the C=C stretching of the quinoid rings at the C=C stretching vibration in the aromatic ring, respectively. The presence of the absorption band at 2515.61 cm^{-1} indicates the presence of hydroxyl groups (-OH) in the composite. These groups may be present on the surface of activated carbon and ZnONPs [41].

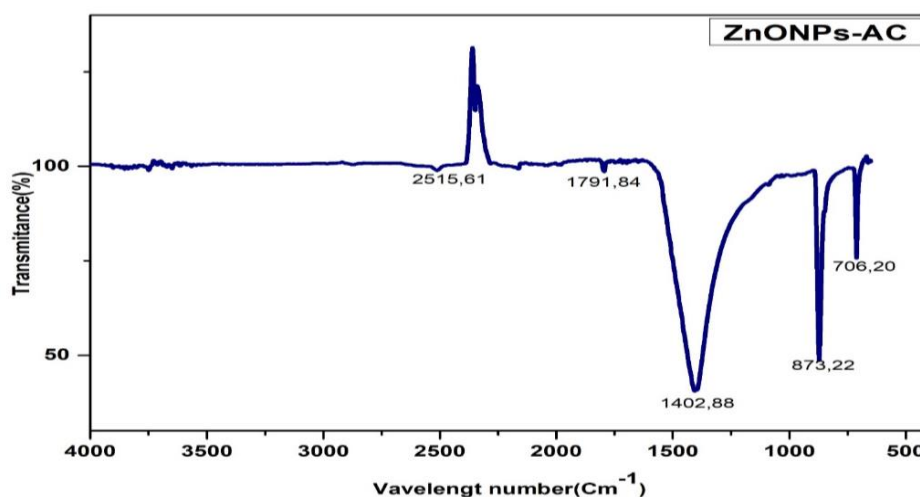


Figure 1: FTIR of ZnONPs- AC

II.1.2. Scanning Electronic Analysis (SEM/EDX)

To study the morphological structure of our composite material (ZnONPs- AC), we carried out a scanning electron microscopy (SEM) analysis. The micrograph in Figure 2 gives us an idea of the textural properties of our composite. From this SEM image, we observe that the small Zinc Oxide nanoparticles (ZnONPs) are homogeneously dispersed on the surface of the activated carbon; a homogeneous dispersion of nanoparticles can improve the activity of the composite. We can see from this micrograph that the ZnONPs have not altered the porous structure of the activated carbon by clogging the pores, but rather are on the surface of the activated carbon. This image also confirms that our material composite has porosity of various sizes, with almost spherical and angular shapes.

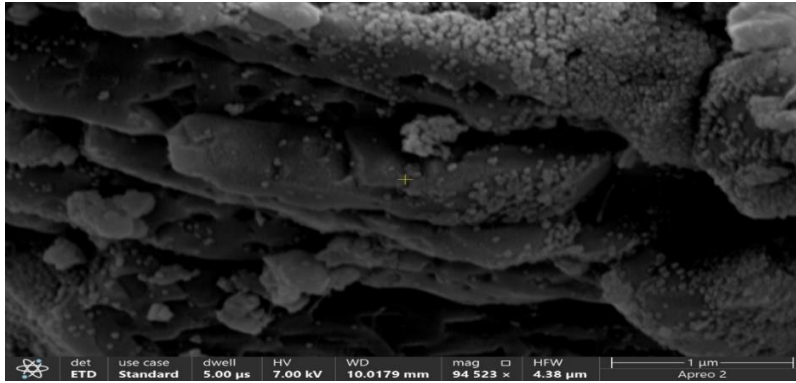


Figure 2: SEM image of ZnONPs-AC

However, to identify and quantify the elements present in our composite, we carried out a complementary analysis, such as energy dispersive (EDX); figure 3 below shows the EDX results for our composite. It revealed that our composite made with activated carbon and zinc oxide nanoparticles is really an assembly of the both. We can see the presence of Zinc and Oxygen plus carbon. Enfact, the presence of Calcium may be due to nature of snail shell.

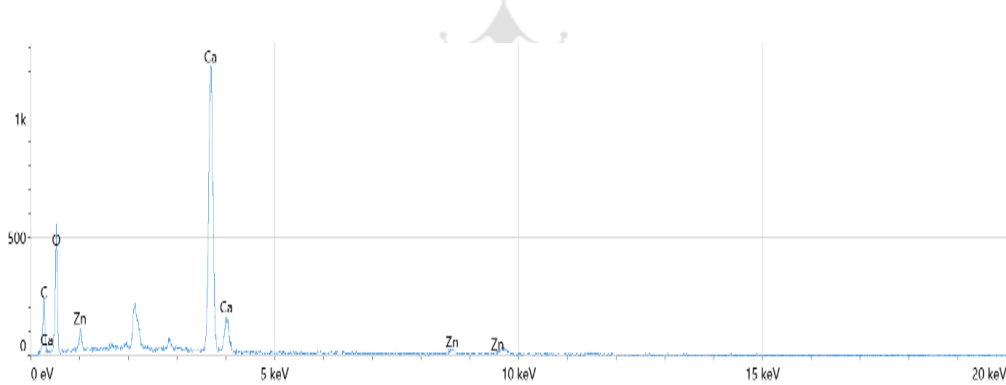


Figure 3 : image de l'EDX du composite (ZnONPs-AC)

The percentages of these elements present in this composite are recorded in table below.

Table 3 : Pourcentages des éléments présents dans le composite (ZnONPs-AC)

Element	Atomic %	Atomic % Error	Weight %	Weight % Error
C	12.4	0.4	7.0	0.2
O	65.4	1.5	49.3	1.1
Ca	20.7	0.2	39.0	0.4
Zn	1.5	0.2	4.6	0.5

II.1.3. X-Ray diffraction analysis

The structural behavior of nanocomposite base of activated carbon landed with zinc oxide nanoparticles (**ZnONPs-AC**) have been determine using X-ray diffraction and reported in figure 4. We can see at 2θ angles of 23.28° ; 29.43° ; 36.03° ; 39.45° ; 43.16° , 47.46° respectively corresponding to (002), (100), (102), (101), (210), (103), (110), (200) with really represent the different crystalline phase of zinc oxide nanoparticles present on the surface of activated carbon. Enfact the activated carbon has been known as non-amorphous, so all those pics are refer to crystallin structure of zinc oxide nanoparticles according to the hexagonal structure of ZnONPs (JCPDS 010891397) [38].

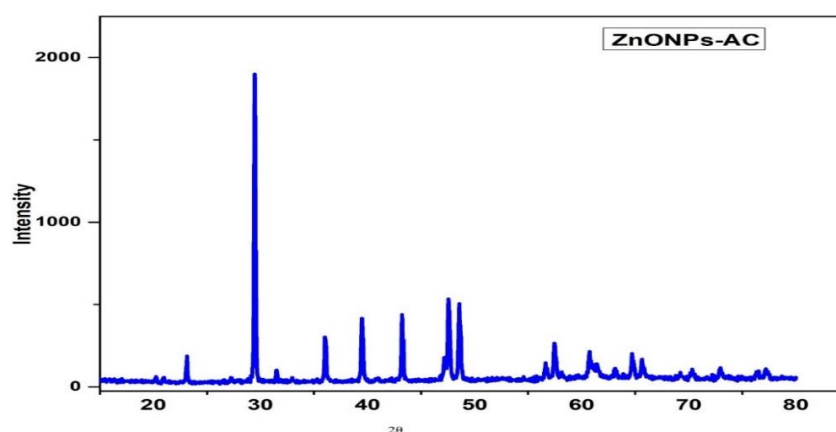


Figure 4: X-Ray analysis of ZnONPs-AC

II.2. Physical characterization of ZnONPs-AC

The adsorption efficiency of a material is also linked to its acid-base character and the reaction medium in which it reacts. To determine the nature of our composite material, we carried out a chemical characterization to determine the pHZPC of our composite. Figure 5 below shows the results of this analysis.

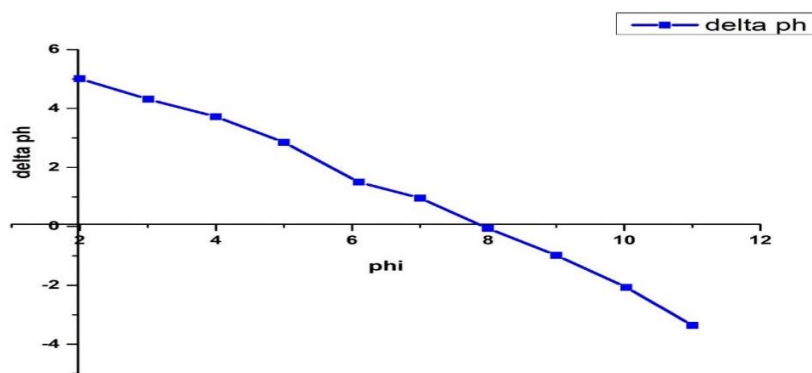


Figure 5: pH at zero charge point (pHZPC) of ZnONPs-AC

We can see from this Figure 5 that the pHZPC of our composite is 8. This means that the material is basic in character. However, at pH values of the yellow 145 solution below pHZPC, our composite will be positively charged due to the excess of H^+ protons in the medium, and the adsorption of anionic species will be favorable due to the strong electrostatic attraction between adsorbent and adsorbate. On the other hand, if the pH of the yellow 145 solution is higher than the pHZPC, the material will be negatively charged due to deprotonation of the acid function present on its surface, and consequently adsorption of cationic species will be favorable because the adsorbent-adsorbate electrostatic attraction will be high [42]. Since reactive yellow 145 is an anionic dye, its adsorption is more favorable in acidic media, since in this medium the **ZnONPs-AC** composite is positively charged and more apt to adsorb anionic species.

In the other hand, immediate analyses have been made for the evaluation of the adsorption capacity of the nanocomposite **ZnONPs-AC**. These analysis revealed an iodine value equal to (IN=888.3 mg/g) with could mean that our material is microporous, as it is well above the 500 mg/g recommended in the literature review by certain authors for activated carbons to be microporous for use in water purification [43]. Indeed, the high MBN elimination rate (93, 69 %) for a material reflects its strong capacity to adsorb medium- and large-sized molecules; this is almost identical to those reported in some previous work [44]. On the basis of the above, we can therefore conclude that **ZnONPs-AC** could be a suitable mesoporous material due to their methylene blue number of 84 mg/g and its elimination rate (93, 69 %).

The moisture and ash content of our composite is low, below 10%. Moisture content is 4%; this low level implies a good material, as the pores are free of water. The ash content of our

composite is 3%; this implies that the pores are completely free of clogging particles [29], thus favouring a high adsorption capacity of **ZnONPs-AC**.

II.3. Adsorption of yellow 145 on composite material

This adsorption is discussed according to parameters such as: contact time, initial concentration, mass of composite, pH of solution and temperature of reaction medium.

II.3.1. Time contact study of the adsorption of yellow 145 on ZnONPs-AC

In order to evaluate the effect of contact time on the adsorption capacity of yellow 145 by **ZnONPs-AC**, a plot of the adsorbed quantity (Q_t) of yellow 145 on prepared composite as a function of time was carried out. The experimental results obtained are shown as follow.

We can see from the figure 6A that the adsorbed quantities of yellow 145 increase with time until they reach a constant value characteristic of the final state of equilibrium between the composite and the molecules present in the yellow 145 solution. It increases from 133.179 mg/g to 150.05 mg/g at contact times of 5 to 120 minutes respectively. We also observe that the curve is subdivided into two parts; the first part corresponds to a very short phase during the first 05 minutes when fixation is very rapid. This could be explained by the high affinity of **ZnONPs-AC** to retain yellow 145 molecules by good internal diffusion through the **ZnONPs-AC** pores. In fact, this period is due to the presence of a large number of free and available adsorption sites on the **ZnONPs-AC** surface during these first minutes [45]. The second part of the curve corresponds to a long phase between 05 and 120 minutes, during which the quantities absorbed increase slightly until they reach a plateau reflecting the final equilibrium state. This may be due to the fact that the diffusion of these pollutant molecules within the pores tends to be cancelled out by the saturation of the adsorption sites [45]. In view of all the above, we set the contact time for the rest of the experiment at 95 minutes, since from this time onwards the adsorbed quantities remained unchanged up to 120 minutes; these adsorbed quantities are of the order of 150.05 mg/g with an adsorption percentage of 90.03%.

II.3.2. Effect of equilibrium concentration

Figure 6B shows that the adsorbed quantity of yellow 145 increases with increasing initial concentration without reaching equilibrium. This can be explained by the availability and non-

saturation of adsorption sites on the surface of the material. Thus, this increase could also be explained by the fact that the increase in the initial concentration of the pollutant leads to the creation of a significant transport force for the molecules of these dyes on the surface of the composite, and as the quantity of molecules present on this surface increases, adsorption becomes more favourable [46]. So, this increase might be attributable to an increase in effective collisions between yellow 145 and adsorbent in solution.

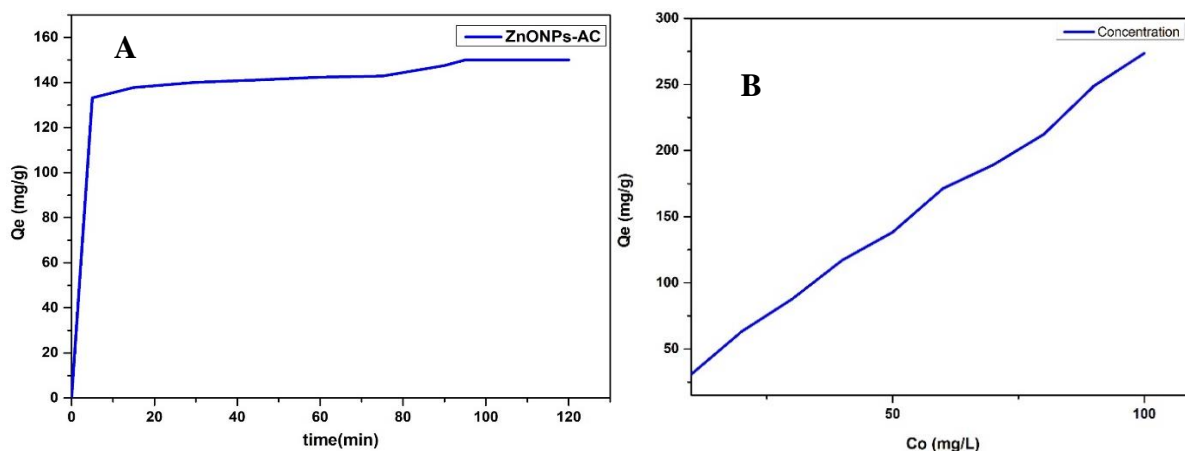


Figure 6A- Influence of contact time on the adsorption capacity of yellow 145 on **ZnONPs-AC**. **B-** Influence of the initial concentration of yellow 145 on **ZnONPs-AC**

II.3.3. Influence of adsorbent mass

The influence of the mass adsorbent was investigated and the adsorbed quantity of yellow 145 on **ZnONPs-AC** is shown in figure below. From this graph we can see that the adsorbed quantities of yellow 145 decrease from 368.87 mg/g to 46.55 mg/g with increasing adsorbent dose (0.01g to 0.1g). This observation provides a simple understanding that the number of available adsorption sites and the surface area of the material decreases with increasing adsorbent mass, resulting in a decrease in the amount of adsorbed material. This could be explained by the fact that as the adsorbent dose increases, the total surface area available for pollutant adsorption decreases, due to a phenomenon known as agglomeration of adsorbent particles at the adsorption sites [47]. Adsorption is therefore at its maximum when the minimum **ZnONPs-AC** content of 0.01g is used, to avoid clogging the active sites with other particles of the material.

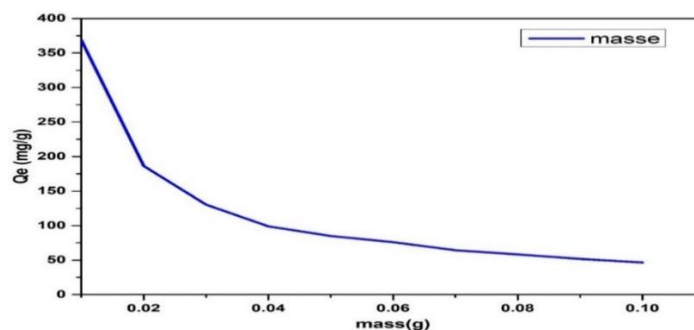


Figure 7: Influence of mass of ZnONPs-AC on the adsorption of yellow 145.

II.3.4. Influence of pH on the retention capacity of yellow 145

Influence of the pH have been done to know at with pH the adsorption will be maximal. We can see that he adsorbed quantities of yellow 145 decrease with increasing pH; for example, at pH= 1 the adsorbed quantity is 156.19 mg/g and at pH= 10 the adsorbed quantity is 51.64 mg/g. The results obtained therefore show that the acidic medium is more favorable to the adsorption of yellow 145 on the material studied than the basic medium. This could be justified by the fact that at pH of the yellow 145 solution lower than $pH_{ZPC} = 8$ ($pH_{solution} < pH_{ZPC}$), the surface of our composite is positively charged and the yellow 145 negatively charged. It should be noted that charges of different natures generate an electrostatic attraction; this favors the adsorption of yellow 145 on **ZnONPs-AC** at low pH values below under 8. On the other hand, the low adsorption capacity of yellow 145 in basic media is justified by the fact that at pH of the yellow 145 solution above $pH_{ZPC} = 8$ ($pH_{solution} > pH_{ZPC}$), the surface of the material is negatively charged and the yellow 145 negatively charged; this charge identity causes electrostatic repulsion, which hinders the adsorption of yellow 145 on **ZnONPs-AC** in these basic pH ranges [47]. Experimental results on the influence of pH on the adsorption capacity of yellow 145 on **ZnONPs-AC** are shown in figure 8 below.

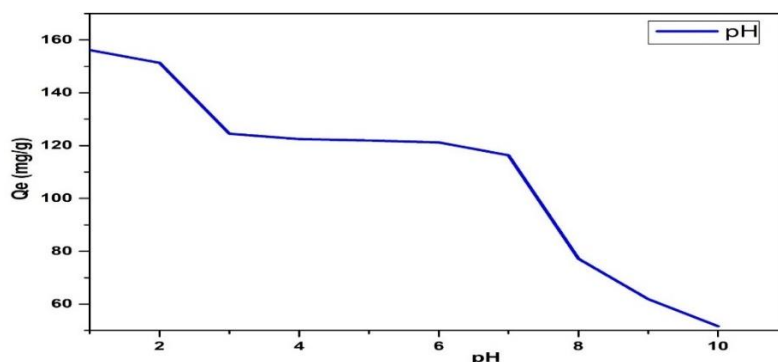


Figure 8: Influence of pH on the adsorption capacity of yellow 145 on ZnONPs-AC

II.3.5. Influence of temperature on adsorption of yellow 145 to ZnONPs-AC

Experimental results on the influence of temperature on the adsorption capacity of yellow 145 on ZnONPs-AC were done and shown in figure 9 below. We can see that the adsorbed quantities of yellow 145 decrease with increasing temperature of the reaction medium; at $T_0 = 35^\circ\text{C}$, the adsorbed quantity is 163.60 mg/g and at $T_0=125^\circ\text{C}$ the adsorbed quantity is 138.30 mg/g. This could be due to the fact that the increase in temperature made the solution of yellow 145 more soluble; and consequently, the more soluble a constituent is in water, the less it adsorbs to activated carbon [48]. In fact, as the temperature rises, ion mobility decreases and thus the diffusion of yellow 145 molecules into the pores of ZnONPs-AC decreases; as a result, yellow 145 molecules have difficulty accessing the active surface sites of ZnONPs-AC [49]. In addition, this decrease in adsorption capacity may be due to the weakening of adsorption forces between the active sites on the adsorbent and the adsorbate species as a result of the destruction of the active sites on the adsorbent by heat [50]. The decrease in the adsorption capacity of yellow 145 with temperature indicates that the process is exothermic, and would under these conditions lead to physical adsorption [51]. Thermodynamic parameters confirm this initial approach. Our experiments were carried out under ambient conditions ($T= 35^\circ\text{C}$).

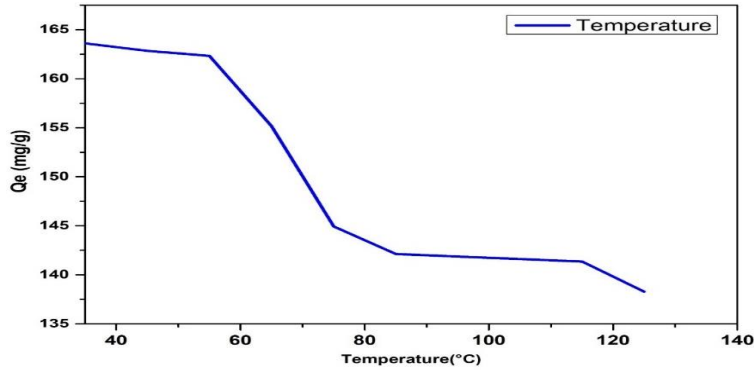


Figure 9: Influence of temperature on the adsorption capacity of yellow 145 on ZnONPs-AC

II.4. kinetics studies of ZnONPs-AC

Pseudo first, second order, Elovich and Intraparticle models were used in this work to explore the adsorption rate. In order to determine the appropriate kinetic model for the adsorption of anionic yellow 145 on ZnONPs-AC, the three kinetic models, namely pseudo-first-order, pseudo-second-order and intraparticle diffusion, were applied to the experimental data obtained during the study of the influence of contact time on the adsorption of this pollutant on our material. The experimental results of each kinetic model for the adsorption of yellow 145 are shown in figure 10 below.

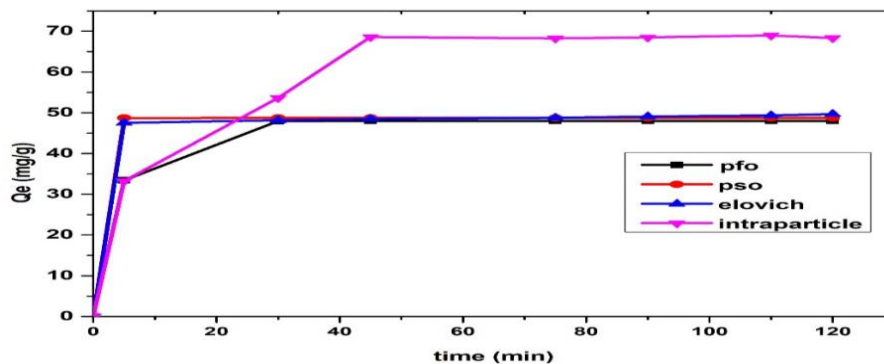


Figure 10: Different kinetic study of ZnONPs-AC to adsorb Yellow 45.

The parameters of these kinetic models, together with the quantities experimentally adsorbed and the values of the difference Δq ($\Delta q = |Q_e \text{ exp} - Q_e \text{ th}|$) between the theoretical (th) and experimental (exp) equilibrium adsorption capacities, are shown in Table 4 below.

Table 4: Yellow 145 adsorption kinetic model parameters on **ZnONPs-AC**.

1er order					2nd Order					Elovich					Intraparticles			
Qe	K ₁	R ²	RMSE	Shi	R ²	RMSE	K ₂	α	β	R ²	RMSE	Shi ²	Kp	cp	rmse	shi ²	R ²	
17.24	1.238	0.98	0.23	0.01	0.99	0.24	28.15	1.011	0.57	0.86	8.24	3.1	4.26	15	25.46	0.01	0.94	

Observation of the values obtained from all these kinetic models, grouped together in Table 3 below, enables us to conclude that the pseudo-second-order kinetic model is the only model that can best describe the adsorption kinetics of yellow 145 on **ZnONPs-AC**; This is justified by its good correlation coefficient ($R^2= 0.99$), which is very close to unity compared with those of the other models, and by the adsorption capacity obtained theoretically (151.52 mg/g), which is very close to the experimental capacity (150.05 mg/g). This closeness of theoretical and experimental values is confirmed by the low value of the difference $\Delta q=1.47$ mg/g between these quantities, thus confirming the reliability of the pseudo-second-order kinetic model compared with all the other models studied [52, 53]. Indeed, the value of the correlation obtained on intraparticle kinetic show that the diffusion of particle is the imminent step rape of yellow 145 in the porosity of **ZnONPs-AC** [54].This could allow us to say that the reactions between the surface functions of our composite located on the grapheme planes and the molecules of this pollutant also control this adsorption process.

II.5. Equilibrium study of ZnONPs-AC adsorption isotherm

In order to better understand the mechanisms of yellow 145 adsorption on our composite, the linear equations of the Langmuir, Freundlich, Tempkin and Dubinin Radushkevich isotherms were used. The experimental results of these isotherms are shown in Figure 11 below.

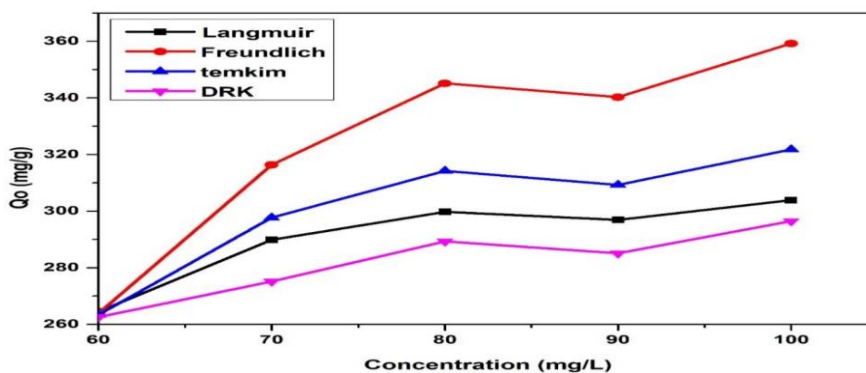


Figure 11: Isotherms for yellow145 adsorption on **ZnONPs-AC** according to the Langmuir, Freundlich, Tempkin and Dubinin-Radushkevich models.

The parameters for each of these isotherms are shown in Table 5 below.

Table 5. Isotherm Parameters

Langmuir					
Qm (mg/g)	KL	RL	R ²	RMSE	Shi ²
351.90277	0.35228607	0.0276025	0.856	52.783	6.876
Freundlich					
KF	1/n	R ²	RMSE	Shi ²	
97.239	0.209	0.998	28.236	12.36	
Dubinin Radushkevich					
Qm	AS	Bs	RMSE	R ²	Shi ²
339.679787	0.24224592	1.84672405	4.42715279	0.99672032	180.362
Tempkin					
b (kJ/mol)	AT (L/T)	B	R ²	RMSE	Shi ²
0.0253	3.682	122.236	0.989	12.56	2.236

From the values recorded in Table 5, we can say that the Freundlich isotherm model best describes the adsorption mechanism of yellow 145 on our composite, with its correlation coefficient 0.99 higher than those of the other isotherm models studied. The equilibrium parameter R_L (or separation factor) of the Langmuir model for the adsorption of yellow 145 is 0.352, indicating that our adsorption is favorable, as $R_L < 1$ and between 0 and 1 [34]. We note from the Freundlich model that the value of $1/nF = 0.209$ is low and the value of n is greater than 1, showing that the adsorption of yellow 145 on our composite is indeed favorable and physical [35]. This result has been confirmed by the less energy obtained D-K-R is better explaining the adsorption process by the determination of the average free energy E (kJ/mol) of sorption which

is free energy that change when one mole of Yellow 145 is fixed on the adsorption surface. According to the result obtained, the adsorption of Yellow 145 is governed by physical adsorption since the free energy E is (1,118 KJ/mol) [49, 36].

II.6. Thermodynamic study

The thermodynamic study of yellow 145 is represented by the plot in figure 12, which gives us the value of the free enthalpy ΔH° and the entropy ΔS° , and by knowing the latter we can determine the free energy ΔG° .

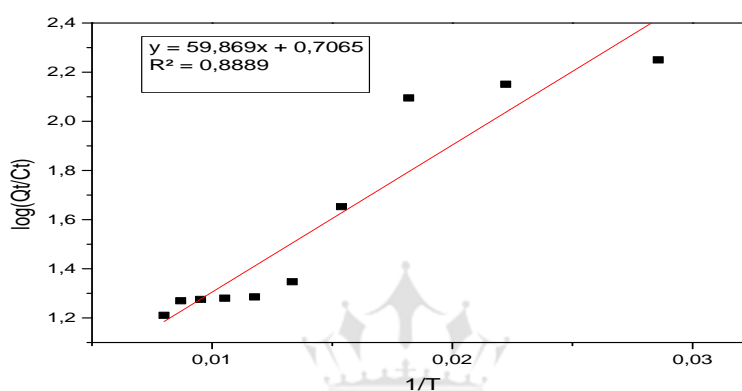


Figure 12: Thermodynamic study of yellow 145 adsorption on ZnONPs-AC

The thermodynamic parameters ΔG° , ΔH° and ΔS° relating to the adsorption of yellow 145 after 95 minutes stirring are grouped in the following Table 6:

Table 6: Thermodynamic parameters ΔG° , ΔH° and ΔS° relating to the adsorption of yellow 145 on ZnONPs-AC.

Matériau	Températures (°K)	ΔG° (KJ/mol)	ΔH° (KJ/mol)	ΔS° (J/mol.K)
ZnONPs-AC	308,15	-4,76	-1,146	0,0135
	318,15	-4,92		
	328,15	-5,08		
	338,15	-5,23		
	348,15	-5,39		
	358,15	-5,54		
	368,15	-5,68		
	378,15	-5,85		
	388,15	-6,00		
	398,15	-6,16		

From these results in Table 6, we observe that the free energy values ΔG° between en - 4.76 and -6.16 KJ/mol at the different temperatures studied are all negative. This could justify the feasibility and spontaneity of the adsorption process of yellow 145 on ZnONPs-AC [55]. The negative value for $\Delta H^\circ = -1.146$ KJ/mol indicates an exothermic adsorption process on the surface of our composite, thus confirming the result of the influence of temperature, where an increase in the temperature of the medium adversely affects the adsorption of yellow 145 on our material. We note that the positive ΔS° value shows that the adsorbed molecules of yellow 145 are not ordered at the solid-solution interface, which is one of the peculiarities of physisorption [56].

Conclusion

The aim of this work was to synthesize a composite material with the best adsorption properties by incorporating zinc oxide on an activated carbon prepared by chemical activation with zinc chloride for yellow 145 reduction in aqueous media.

The $pHZPC = 7.93$ value shows that the surface of our prepared ZnONPs-AC is much more basic; at this $pHZPC$ value, adsorption of yellow 145 is favored in acidic media because in this medium the material is positively charged and able to adsorb anionic yellow 145. The iodine value (862.92 m^2/g) and methylene blue elimination rate (93.69%) confirm the heterogeneity of ZnONPs-AC pores. The good correlation coefficient $R^2 = 0.99$ of the pseudo-second-order kinetic model show that this model better describes the yellow 145 adsorption process on

ZnONPs-AC. The high value of the R^2 on intraparticle kinetic show that the diffusion of the particles is the best rate of Yellow 145 in the porosity of ZnONPs-AC. In addition, the Freundlich model's acceptable correlation coefficient $R^2= 0.99$ compared with those of the other models, it provides a better description of yellow 145 adsorption on our composite. And DRK show that the adsorption was determined by physical phenomenon. The thermodynamic study yielded negative values for the free energy ΔG° (ranging from -4.76 KJ/mol to -6.16 KJ/mol); this justifies the feasibility and spontaneity of the adsorption process of yellow 145 on ZnONPs-AC; in addition, the value of the free enthalpy being also negative ΔH° (-1.146 KJ/mol) translates an exothermic adsorption on the surface of our composite. The positive value of ΔS° (0.0135 J/mol.K) shows that the adsorbed molecules of yellow 145 are not ordered at the solid-solution interface. The ZnONPs-AC was found to be semicrystalline and with a variety of porosity such as micro and mesoporosity.

REFERENCES

- [1] Oteng. A, Smout. M, Yankson. I, (2017). Poverty politics and governance of potable water services: The core-periphery syntax in Metropolitan Accra, Ghana. *Urban Forum*, vol 2. Springer, pp185–203.
- [2] Bougherira. N, Hani. A, Toumi. F, et al, (2017). Impact des rejets urbains et industriels sur la qualité des eaux de la plaine de la Meboudja (Algérie). *Hydrological Sciences Journal*;62:1290–1300.
- [3] Bouacherine. S, (2013). Eliminations des polluants spécifiques par adsorption sur charbon actif et argile traitée et non traitée, mémoire de master, Université Mohamed Chérif Messaadia –Souk-Ahras, p 1.
- [4] Encyclopaedia Universalis, les colorants, 2003
- [5] Rehn .L, Blasengeschwulste bei Fuschin arbeiten. *Arch. Klein Chir*, 50 (1895) 588.
- [6] Tsuda. S, Matsusaka. N, Madarame. H,(2000). the comet assay in eight mouse organs: result with 24 azo compounds. *Mutation Research*, 465 11-26.
- [7] Morin-Crini. N, Crini. G (eds) (2017) *Eaux industrielles contaminées*. PUFC, Besançon
- [8] Zakaria. M; (2018) ; Synthèse de nanoparticules magnétiques fonctionnalisées Application pour la complexation de métaux; Thèse de Doctorat LMD en CHIMIE Moléculaire et Environnement ; université d'ORAN; P1.
- [9] Sun. J, Wang. J, Zhang. R, Wei. D, Long. Q, Huang. Y (2017) *Chemosphere Comparison of different advanced treatment processes in removing endocrine disruption effects from municipal wastewater secondary effluent*. *Chemosphere* 168:1–9.
- [10] Atkins. P.W, (1994). *Physical chemistry*, 5Th Edition, Oxford University press, Oxford, 25-30.
- [11] Guechi el. K, (2013). "Enlèvement de colorants à partir de solutions aqueuses par des matériaux sorbants non conventionnels et à faible coût". *Génie Chimique. Mémoire de thèse Université Badji Mokhtar-Annaba*, 64, 1-26.
- [12] S. Jeddi. A, Ouassini. M, El Ouahaby. H, Mghafri, (2016) Valorisation of natural mineral substances (NMS) at adsorption techniques: case of olive oil mill waste waters, *J. Mater. Environ. Sci.* 7 (2) 488–496.
- [13] Kouotou. D, Manga. H.N, Baçaoui. A, Yaacoubi.J.K, Mbadcam. J, (2013). Optimization of activated carbons prepared by and steam activation of oil palm shells
- [14] Dimitrios. K, Sophia. B, Panagiota. P, Evan. D, (2008). Production of activated carbon from bagasse and rice husk by a single-stage chemical activation method at low retention time, *Bioresource Technology*.

- [15] Slokar. Y. M, Marechal. L. E, (1998). A Methods of Decoloration of Textile wastewaters. Dyes and Pigments, 37, p 335-356.
- [16] Malik. R, Ramteke. D. S, Wate. R. S, (2007). Adsorption of malachite green on groundnut shell waste based powdered activated carbon. 1129-1138.
- [17] Tomas. K. V, Fileman. T. W, Readman. J. W, (2001). Antifouling paint biocides in the UK Coastal environment and potential risks of biological effects, 42, p 677 – 688.
- [18] Jagoret. P, (2019) L'agroforesterie: des pratiques diversifiées pour la transition agro- écologique du cacao culture africaine, La transition agro-écologique p59.
- [19] L. Wu, L. Liao, G. Lv, F. Qin, Y. He, X. Wang, (2013) Micro-electrolysis of Cr (VI) in the nanoscale zero-valent iron loaded activated carbon, J. Hazard. Mater. 254 277–283.
- [20] J. Nga, J. Avom, J. Tonga Limbe, D. Ndinteh, H.L. Assonfack, C.M. Kede, Kinetics and thermodynamics of β -carotene adsorption onto acid-activated clays modified by zero valent iron, J. Chem. (2022) 1–15.
- [21] Masoudian N, Rajabi M, Ghaedi M (2019) Titanium oxide nanoparticles loaded onto activated carbon prepared from bio-waste watermelon rind for the efficient ultrasonic-assisted adsorption of congo red and phenol red dyes from wastewaters. Polyhedron 173:114105.
- [22] Choina. J, (2015) the influence of the textural properties of ZnO nanoparticles on adsorption and photocatalytic remediation of water from pharmaceuticals. Catal Today 241:47–54.
- [23] Deb A, Kanmani M, Debnath A, Bhowmik KL, Saha B (2019) Ultrasonic assisted enhanced adsorption of methyl orange dye onto polyaniline impregnated zinc oxide nanoparticles: kinetic, isotherm and optimization of process parameters. Ultrason Sonochem 54(January):290–301.
- [24] Sridhar R, Ramanane UU, Rajasimman M (2018) ZnO nanoparticles – synthesis, characterization and its application for phenol removal from synthetic and pharmaceutical industry wastewater. Environ Nanotechnol Monit Manag 10:388–393.
- [25] Mohammed AA, Al-Musawi TJ, Kareem SL, Zarrabi M, Al- Ma'abreh AM (2019) Simultaneous adsorption of tetracycline, amoxicillin, and ciprofloxacin by pistachio shell powder coated with zinc oxide nanoparticles. Arab J Chem 13(3):4629–4643.
- [26] Bolver G, Bedia J, Gómez-Avilés A, Peñas-Garzón M, Rodriguez JJ (2019) Semiconductor photocatalysis for water purification. Nanoscale Mater Water Purif.
- [27] Udeozor S. O , Evbuomwan B. O (2014), The Effectiveness of Snail Shell as Adsorbent For The Treatment of Waste Water From Beverage Industries Using H₃ Po₄ As Activating Agent, IOSR Journal of Engineering (IOSRJEN), 2250-3021, ISSN (p): 2278-8719 Vol. 04, ||V1|| PP 37- 41
- [28] N. Djebri, N. Boukhalifa, M. Boutahala, N. Chelali, (2017), Préparation des biomatériaux d'hydrogels à base d'argile et d'alginate (algues brunes): application environnementale. Algérie. Journal of Environmental Science and Technology
- [29] Ousmaila Sanda. M, Adamou. Z, Ibrahim. D, Ibrahim. N, (2016) “Préparation et caractérisation de charbons actifs à base de coques de noyaux de BalanitesEagyiatica et de Zizyphus Mauritiana“. Journal de la Société Ouest-Africaine de Chimie, 041 : 59 – 67
- [30] Jacques Bomiko M, Caroline Lincold Nintedem M, Pierre Gerard T*, Harlette Zapenaha P, (2021), Adsorption of Chromium (VI) onto Activated Carbons Prepared from Raphia farinifera Fruit Kernels by Chemical Activation with Phosphoric Acid (H₃PO₄), International journal of science ,Research methodology, www.ijsrm.humanjournals.com
- [31] Tay. J. H, Chen. X. G, Jeyaseelan. S, Graham. N, (2001). Optimising the preparation of activated carbon from digested sewage sludge and coconut husk, Chemosphere 44, 45 –51.
- [32] Auta.M, Ameen.B.H, (2011), Optimized waste tea activated carbon for adsorption of Methylene Blue and Acid Blue 29 dyes using response surface methodology, Chem. Eng. J. 175 233–243.
- [33] H. Tounsadi, A. Khalidi, M. Abdennouri, N. Barka, (2016), Activated carbon from Diplotaxis Harra biomass: optimization of preparation conditions and heavy metal removal, J. Taiwan Inst. Chem. Eng. 59 348–358

- [34] Dada, A.O, Olalekan, Olatunya A.P, DADA A.M, (2012). Langmuir, Freundlich, Temkin and Dubinin–Radushkevich Isotherms Studies of Equilibrium Sorption of Zn²⁺ Phosphoric Acid Modified Rice Husk. Journal of Applied Chemistry.
- [35] BENAMRAOUI. F, (2014). Elimination des colorants cationiques par des charbons actifs synthétisés à partir des résidus de l’agriculture. Mémoire Magister, Option: Génie Chimique, Université Ferhat Abbas Setif-1 UFAS (ALEGERIE).
- [36] Gładysz-P, Agnieszka, (2017).Application of modified clay for removal of phenol and PO₄³⁻ ions from aqueous Solutions. Adsorption Science & Technology .2017, Vol. 35(7–8) 692–699.
- [37] Colak. N, Atar. A, Olgun.C, Eng. J, (2009). Bio sorption of acidic dyes from aqueous solution by *Paenibacillus macerans* : kineti, thermodynamic and equilibrium studies, 150 p
- [38] Karthik R, Thambidurai S (2017) Synthèse de nano tiges de ZnO/oxyde de graphène réduit dopé au cobalt comme matériau actif pour le capteur d’ions de métaux lourds et l’activité antibactérienne. J Alloys Compd. 715: 254265.
- [39] Zhang. L, Zhang. Q, (2015), Synthesis and characterization of novel ZnO/activated carbon nanocomposites for efficient photocatalytic degradation of methylene blue. Journal of Alloys and Compounds, 647, 827-835.
- [40] Wang. Z. L, Kang. Z. H, (2018), Functional and nanostructured materials for energy and environmental applications.
- [41] Li. Y, Zhang. L, (2023), recent advances in the synthesis and application of ZnO/activated carbon composites for environmental remediation: a review. Journal of Hazardous Materials, 442, 126470.
- [42] Eldeeb.T.M, Aigbe.U.O, Ukhurebor.K.E, Onyancha.R.B, El-Nemr.M.A, Hassaan.M.A, Osibote.O.A, Ragab.S, Okundaye.B, Balogun.V.A, El Nemr.A, (2022) Bio sorption du colorant acide brun 14 en man-darin biochar-CO-TETA issu d’écorces de mandarine. Conversations sur la biomasse Biorefne, 1–2.
- [43] Aravindhan.R, Nair.B.U, (2009). “Preparation and characterization of activated carbon from marine macro-algal biomass“. Journal of Hazardous Materials, 162, 688–694
- [44] Tchieta, P. G., Mbouombouo, J. B, Caroline.L. N. M, Charles.M. K, Harlette, P. Z. (2019). Adsorption of Eriochrome Black T (EBT) Onto Activated Carbons Obtained from Cola Anomala Nut Shells by Chemical Activation with Phosphoric Acid (H₃PO₄), international Journal of Science and Research, 8, 2319-7064.
- [45] Hamzeh. Y, Ashori. A, Azadeh. E, Abdulkhani. A, (2012). Removal of acid Orange 7 and remazol black 5 reactive dyes from aqueous solutions using a novel bio sorbent; Mater. Sci. Eng, 32, 1394–1400.
- [46] Girish.C.R, Victoria. R.M, (2014). Adsorption of Phenol from Aqueous Solution Using Lantana camara, Forest Waste: Kinetics, Isotherm, and Thermodynamic Studies. International Scholarly Research Notices, ID 201626, 16.
- [47] Das B, Mondal N.K., (2011). “Calcareous soil as a new adsorbent to remove lead from aqueous solution: equilibrium, kinetic and thermodynamic study,” Univ. J. Environ. Res. Technol., 1(4), 515-530.
- [48] Alvarez. P. M, Garcia-Araya. F. J, Beltran. F. J, (2005). Ozonation of activated carbons: effect on the adsorption of selected phenolic compounds from aqueous solutions, J. Colloid Interface Sci, 283, 503–512.
- [49] Khoulalene. L, Semmar. S, (2016). Étude Cinétique et Thermodynamique de l’Adsorption du Noir Erichrome T sur le Charbon. Memoire de Master Université A. Mira-Béjaia, 89.
- [50] Abdelwahab.O, Amin.N.K, (2013). Adsorption du phénol à partir de solutions aqueuses par les fibres de *Luffa cylindrica*: études cinétiques, isothermes et thermodynamiques. Journal égyptien de la recherche aquatique 39, 215–223
- [51] YAHIAOUI N (2012). Etude de l’adsorption des composés phénoliques des margines d’olive sur carbonate de calcium, hydroxyapatite et charbon actif. Mémoire de magister en chimie, option chimie de l’environnement, université de TIZI OUZOU, pp : 33-45.
- [52] Li. Z, Chang. P.H, Jiang. W.T, Jean. J.S, Hong. H, (2011). Mechanism of methylene blue removal from water by swelling clays. Chemical Engineering Journal, 168:1193-1200.
- [53] Dawood. S, Sen. T. K, (2012). Removal of anionic dye congo red from aqueous solution by raw pine and acid-treated pine cone powder as adsorbent: Equilibrium, thermodynamic, kinetics, mechanism and process design. Water Research, 46:1933-1946.

- [54] Kataria. N, Garg. V. K, Jain. M, Kadirvelu. K, (2016). Preparation, characterization and potential use of flower shaped Zinc oxide nanoparticles (ZON) for the adsorption of Victoria Blue B dye from aqueous solution. *Adv. Powder Technol.*, 27, 1180-1188.
- [55] Noura A.S. Mohammeda, Rund A. Abu-Zurayk, Imad Hamadneh, Ammar H. Al-Dujaili, (2018). Phenol adsorption on biochar prepared from the pine fruit shells:Equilibrium, kinetic and thermodynamics studies. *Journal of Environmental Management*.
- [56] Aarfane.A, Salhi.A , El Krati.M ,Tahiri.S , Monkade.M ,Lhadi.E.K, Bensitel.M, (2014). Kinetic and thermodynamic study of the adsorption of Red195 and Methylene blue dyes on fly ash and bot. *J. Mater. Environ. Sci.* 5 (6) 1927-1939.

